Available online at www.sciencedirect.com
ScienceDirect
Polymer 48 (2007) 910–916
polymer
www.elsevier.com/locate/polymer

Molecular basis behind the substrate specificity of polygalacturonase through computational study

S.M. Malathy Sony, M.N. Ponnuswamy*

Department of Crystallography and Biophysics, University of Madras, Guindy campus, Chennai 600025, Tamilnadu, India

Received 11 August 2006; received in revised form 16 November 2006; accepted 20 November 2006
Available online 20 December 2006

Abstract

Polygalacturonases (PGs) hydrolyze the pectins present in the cell walls of higher plants. PGs prefer pectic acid rather than pectins as substrate and methylesterification of pectic acid is known to inhibit the activity of fungal PG. In order to identify the molecular basis of the differential specificity towards the substrates, octagalacturonic acid and its methylesterified derivative are flexibly docked with tomato PG and fungal PG. The substrate octagalacturonic acid is found to bind with the non-reducing end towards the N-terminus of PG whereas its methylesterified derivative binds in opposite direction with both the PGs. Both methylesterified derivative complexes did not show the catalytically important Asp residue in the interaction map suggesting strongly the inactiveness of the PGs with the methylesterified substrate. The tomato PG–octagalacturonic acid complex possesses stronger interaction when compared to its methylesterified substrate whereas it is the methylesterified substrate, which shows stronger interaction in the fungal PG explaining its inhibition mode.

Keywords: Polygalacturonase; Pectins; Galacturonic acid

1. Introduction

Polygalacturonases (PGs) hydrolyze the α-(1,4)-glycosidic bonds between adjacent galacturonic acid residues and release oligogalacturonides. They are classified as *endo*-PGs and *exo*-PGs, according to their mode of action [1]. PGs are classified as the family 28 of glycosyl hydrolases based on amino acid sequence similarity [2–4]. Pickersgill and coworkers [5] performed sequence alignment of *endo*-PGs that revealed four conserved regions: Asn-Thr-Asp, Gly-Asp-Asp, Gly-His-Gly, and Arg-Ile-Lys and this clustering indicates the functional conservation. Based on sequence analysis it was found that eight residues are strictly conserved [6] and site-directed mutagenesis study in fungal PGs suggested that three Asp residues (180, 201, and 202; numbered with respect to *Aspergillus niger* endopolygalacturonase II) are directly involved in catalysis, Arg (256) and Lys (258) residues in substrate binding and a His residue (223) in maintaining the proper ionization state of the catalytic Asp [7].

PGs are of inverting type i.e., the glycosidic linkages are hydrolyzed by a single displacement mechanism with inversion in anomeric configuration [8]. Glycosidases have a pair of carboxylic acid groups at the active site; one acting as a general acid donating a proton to the glycosidic oxygen of the scissile bond and the other as a general base which activates a water molecule that performs a nucleophilic attack on the anomeric carbon of sugar. In inverting enzymes these two residues are approximately 10 Å apart but crystal structure analysis of *endo*-PGs showed them to be only 5.6 Å apart suggesting that the protonation of the glycosidic oxygen and nucleophilic attack at the anomeric carbon are at the same side of the bond in α-linked polysaccharides [5,9]. This suggested mechanism could be confirmed either by a three-dimensional structure of an enzyme–substrate complex or a high-resolution structure with substrate modeled to a high accuracy. In this study the latter approach was adopted to understand the influence of the functional clusters [5] and the conserved residues [6] of the PG family in substrate binding through docking.

* Corresponding author. Tel.: +91 44 2235 1367; fax: +91 44 2230 0122.
E-mail address: mnpsy2004@yahoo.com (M.N. Ponnuswamy).

0032-3861/$ - see front matter © 2006 Elsevier Ltd. All rights reserved.
doi:10.1016/j.polymer.2006.11.055

Table 1
Dataset used for the sequence analysis of polygalacturonases

Entry name	AC	Organisms	Length (no. of residues)
PGLR1_ASPAC	O74213	*Aspergillus aculeatus*	378
PGLR1_ASPNG	P26213	*Aspergillus niger*	368
PGLR1_COLLN	Q00446	*Colletotrichum lindemuthianum* (Anthracnose fungus)	363
PGLR1_ERWCA	P18192	*Erwinia carotovora*	402
PGLR1_PENOL	Q9Y834	*Penicillium olsonii*	370
PGLR1_RALSO	P58598	*Ralstonia solanacearum* (*Pseudomonas solanacearum*)	531
PGLR1_SCLSC	Q12708	*Sclerotinia sclerotiorum*	380
PGLR2_ASPNG	P26214	*A. niger*	362
PGLR2_ASPTU	P19805	*Aspergillus tubingensis*	362
PGLR2_CHAOB	Q7M1E7	*Chamaecyparis obtusa* (Japanese cypress)	514
PGLR2_CRYJA	P43212	*Cryptomeria japonica* (Japanese cedar)	514
PGLR2_ERWCA	P26509	*E. carotovora*	402
PGLR2_JUNAS	Q9FY19	*Juniperus ashei* (Ozark white cedar)	507
PGLR2_PENOL	Q9Y833	*P. olsonii*	380
PGLR2_RALSO	P20041	*R. solanacearum* (*P. solanacearum*)	529
PGLR3_ASPNG	Q12554	*A. niger*	383
PGLR4_ASPNG	O42809	*A. niger*	378
PGLRA_ASPFL	P41749	*Aspergillus flavus*	363
PGLRB_ASPFL	P41750	*A. flavus*	366
PGLR_ACTCH	P35336	*Actinidia chinensis* (Kiwi) (Yangtao)	467
PGLR_AGRTU	P27644	*Agrobacterium tumefaciens*	312
PGLR_ASPOR	P35335	*Aspergillus oryzae*	363
PGLR_ASPPA	P49575	*Aspergillus parasiticus*	363
PGLR_BRANA	P35337	*Brassica napus* (rape)	397
PGLR_COCCA	P26215	*Cochliobolus carbonum* (*Bipolaris zeicola*)	364
PGLR_GIBFU	Q07181	*Gibberella fujikuroi* (bakanae and foot rot disease fungus) (*Fusarium moniliforme*)	373
PGLR_GOSBA	Q39766	*Gossypium barbadense* (sea-island cotton) (Egyptian cotton)	407
PGLR_GOSHI	Q39786	*Gossypium hirsutum* (upland cotton)	407
PGLR_LYCES	P05117	*Lycopersicon esculentum* (tomato)	457
PGLR_MALDO	P48978	*Malus domestica* (apple) (*Malus sylvestris*)	460
PGLR_MEDSA	Q40312	*Medicago sativa* (Alfalfa)	421
PGLR_PENDI	Q9Y718	*Penicillium digitatum*	367
PGLR_PENEN	O59925	*Penicillium expansum*	378
PGLR_PENGR	O93883	*Penicillium griseoroseum*	376
PGLR_PENJA	O42824	*Penicillium janthinellum* (*Penicillium vitale*)	371
PGLR_PERAE	Q02096	*Persea americana* (avocado)	462
PGLR_PRUPE	P48979	*Prunus persica* (peach)	393
PGLR_TOBAC	Q05967	*Nicotiana tabacum* (common tobacco)	396
PGLR_YEAST	P47180	*Saccharomyces cerevisiae* (baker's yeast)	361

It has been reported that methylesterification is known to inhibit the activity of fungal PG more than plant PG and the substrate specificity study demonstrated that polygalacturonase preferred pectic acid rather than pectins as substrate [10]. Therefore in order to understand the substrate preference, octagalacturonic acid (PGA) and its methylesterified derivative (PGM) were docked to tomato PG (modeled structure; since no plant PG structures are available yet) and fungal PG (PDB ID: 1czf). The results obtained were then correlated with the enzymatic activity of PG on the substrate.

2. Methodology

2.1. Sequence analysis

The sequences of known PGs were extracted from the Carbohydrate-Active Enzymes (CAZy) database [11] and only Swiss-Prot database entries were used for the analysis. Multiple sequence analysis was carried out using CLUSTALW program [12] version 1.83 and few manual adjustments to the alignment were also made.

2.2. Three-dimensional structure prediction of tomato PG

The Swiss-Prot accession number for the sequence that was used for constructing the model of tomato PG is P05117 and the matured protein has 386 residues [13]. Search for homologous structures to be used as template by BLAST server yielded five β-helical proteins (1bhe, 1nhc, 1czf, 1hg8 and 1ib4) with similar scores, 41–47% sequence similarity. Superposition using the viewer program Deepview/Swiss-PDB Viewer, Release 3.7 (SP3) and secondary structure calculation carried out by DSSP program [14] showed that the five templates are structurally very similar with the RMS deviation being within 1.6 Å and the percentage secondary structure identity being more than 80%. It was inferred from these

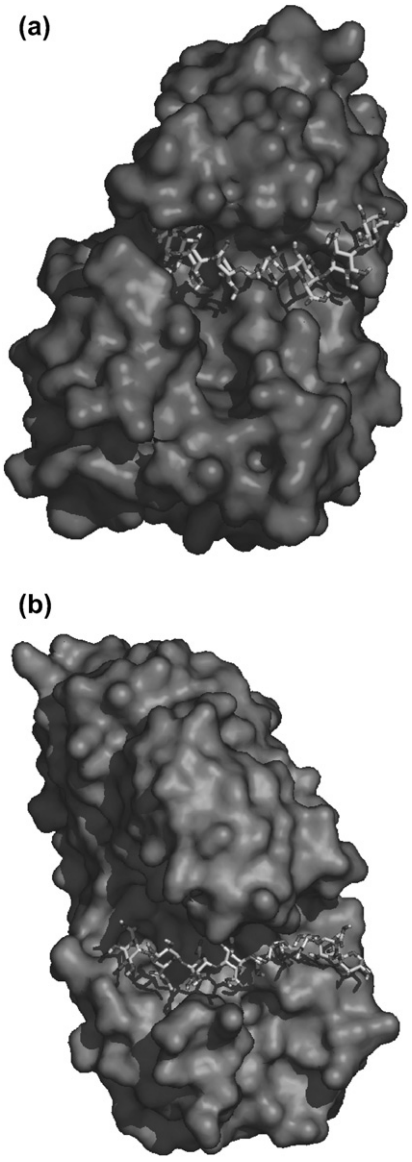

Fig. 1. The modeled structure of the (a) tomato polygalacturonase with octagalacturonic acid and (b) fungal polygalacturonase with methylesterified derivative of octagalacturonic acid. The surface representation and the substrate binding (stick model) of the protein are shown. The N-terminus of the protein is on the top and the C-terminus is on the bottom.

analyses that no single structure could be chosen as superior than the other, and therefore all of them were chosen to perform a profile-based analysis. In this analysis structure based sequence alignment for all the template structures was carried out using STAMP software [15] and based on this structural alignment an average structure was constructed and this model was chosen as the template for structure prediction (Fig. S1 in Supplementary data). For this model the side chains are built using the Biopolymer module of the INSIGHTII package of BIOSYM [16]. The loop regions were constructed using both INSIGHTII and Swiss-PDB Viewer packages. This model was then submitted to the Optimise mode of the Swiss-Model server [17] for structure optimization, which performs energy minimization and molecular dynamics to remove steric

Table 2
Bond angle [τ (°)] and backbone torsion angles [ϕ (°) and ψ (°)] about glycosidic bonds in the modeled structure of the polygalacturonase–octagalacturonate complexes

	Initial model						Complex with tomato PG						Complex with fungal PG					
	PGA			PGM			PGA			PGM			PGA			PGM		
	τ	ϕ	ψ	τ	ϕ	ψ	τ	ϕ	ψ	τ	ϕ	ψ	τ	ϕ	ψ	τ	ϕ	ψ
$GalpA^{-4}$–$GalpA^{-3}$	116.9	71.7	103.4	116.8	67.9	105.3	117.0	157.9	160.2	116.8	74.4	124.9	116.9	160.5	143.0	116.8	148.8	150.7
$GalpA^{-3}$–$GalpA^{-2}$	117.8	75.6	100.5	116.9	75.2	101.7	117.8	101.5	−44.2	117.0	128.6	155.4	117.8	120.6	150.6	117.0	89.0	143.7
$GalpA^{-2}$–$GalpA^{-1}$	120.1	64.5	135.1	119.0	60.9	127.5	120.2	−26.5	113.1	119.0	68.2	123.9	120.1	140.6	−170.5	119.0	−35.1	103.7
$GalpA^{-1}$–$GalpA^{+1}$	118.0	70.4	102.6	117.8	66.3	102.8	118.0	92.2	−177.8	117.8	78.5	107.7	117.9	96.2	167.7	117.8	64.5	93.1
$GalpA^{+1}$–$GalpA^{+2}$	117.9	79.3	130.5	118.2	80.1	139.6	117.8	156.9	161.6	118.2	108.4	159.9	117.8	66.2	122.5	118.2	89.2	165.7
$GalpA^{+2}$–$GalpA^{+3}$	118.4	81.0	133.8	118.6	82.1	141.4	118.4	109.1	−173.1	118.5	175.5	154.6	118.3	79.3	141.1	118.6	71.7	67.9
$GalpA^{+3}$–$GalpA^{+4}$	117.3	71.7	102.5	117.0	67.6	105.7	117.4	171.2	141.6	117.0	72.5	70.1	117.3	21.6	109.9	117.0	163.9	161.4

Note: bond angle $\tau = (C1_i–O_{i+1}–C4_{i+1})$, torsion angles $\phi = (OR_i–C1_i–O_{i+1}–C4_{i+1})$ and $\psi = (C1_i–O_{i+1}–C4_{i+1}–C5_{i+1})$. Torsion angles are determined by looking from the non-reducing end side (i) down the bond of interest to the reducing end side (i + 1).

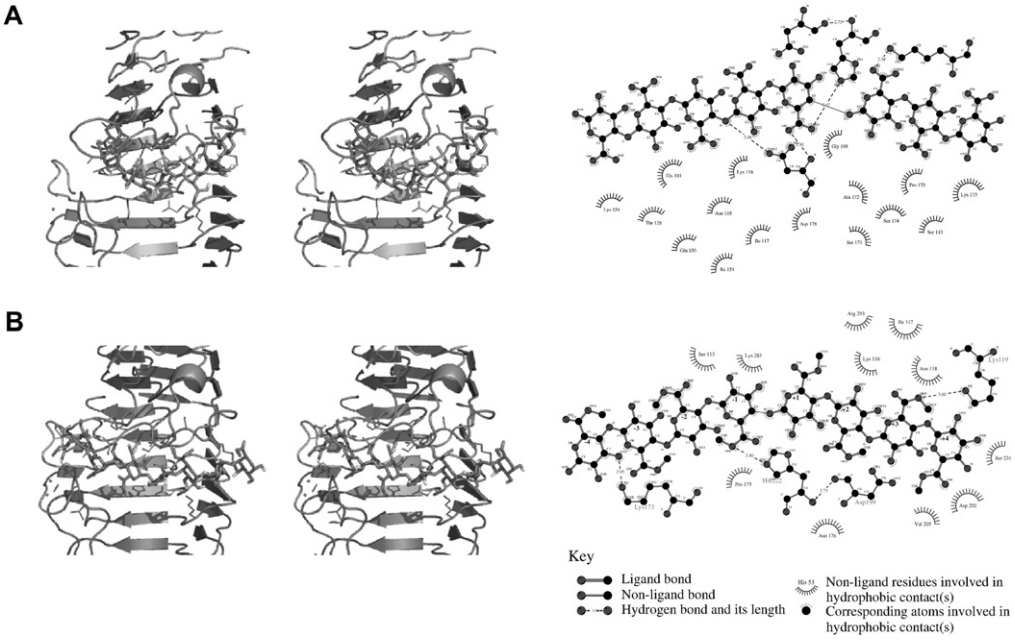

Fig. 2. Stereo plot of the protein (cartoon representation)–ligand (stick representation) complexes and their corresponding ligplot showing the detailed interaction mode between the amino acid residues of tomato PG with (A) PGA and (B) PGM residues.

clashes. The model was verified using WHATCHECK [18] program and Ramachandran plot which showed minimum abnormalities (taking into account only the non-glycine and non-N or non-C-terminal residues, 86% of the residues in the most favored regions and the remaining residues in the additionally allowed regions) indicating the structure to be stereochemically good.

2.3. Docking studies

The octagalacturonic acid, eight monomer units of α-D-galacturonic acid (GalpA) joined through 1-4 linkage, was built using the modeling kit of the SWEET (Program 2) database as an unbent irregular helix. The monomer of this modeled octagalacturonic acid (PGA) is named starting from +4 through +1, −1 through −4. The pyranose ring of the $GalpA^{-1}$ residue of PGA has a half-chair ($^4H_3$) form while other rings have a relaxed chair ($^4C_1$) form. The geometrical arrangement of the catalytically important three Asp residues in the crystal structure required $GalpA^{-1}$–$GalpA^{+1}$ segment to be in a strained conformation if both the rings adopt relaxed chair form and therefore the pyranose ring of $GalpA^{-1}$ residue is proposed to have high energy form [19,20]. This substrate distortion at −1 subsite is important for the stabilization of the oxocarbenium-ion-like transition state [21]. Various forms such as chair, twist-boat and half-chair were considered for the $GalpA^{-1}$ residue in this study but only the half-chair form produced biochemically suitable model. This model of PGA was optimized by constrained energy minimization using AMBER force field available in the DISCOVER tool of the Insight II package of BIOSYM.

The substrate model was then flexibly docked, the backbone torsion angles $\phi = (OR_i–C1_i–O_{i+1}–C4_{i+1})$ and $\psi = (C1_i–O_{i+1}–C4_{i+1}–C5_{i+1})$ of the PGA were allowed to vary, to the predicted structure of tomato PG and the crystal structure of fungal PG (A-chain of 1czf). AutoDOCK program version 3.0.5 [22] was used for this docking. Water molecules were not used for the docking studies as it makes the analysis complicated. Twenty-five best configurations of the protein–ligand complexes were retrieved and the one that supports the biochemical studies was chosen. The hydrogen bond and non-bonded contacts for the complexes were calculated using the program HBPLUS [23] and the pictorial representations are drawn using the program LIGPLOT [24].

3. Results and discussion

3.1. Identification of functional clusters in PGs

In order to ascertain once again the role of functional clustering sequence analysis of all PGs from different species was carried out. The Swiss-Prot entries are presented in Table 1. Multiple sequence alignment (Fig. S2 in Supplementary data) yielded five major clusters, Asn-Thr-Asp, Asp-Asp, Gly-His-Gly, Ser-Ile-Gly-Ser, Arg-Ile-Lys, and these clustering indicates the functional conservation. Pickersgill and coworkers [5] did not detect Ser-Ile-Gly-Ser cluster that was identified in this analysis. In addition in the second cluster they proposed a Gly residue before Asp-Asp but this residue differs according to speciation. In bacterial and plant PGs, Gly residue is conserved whereas in fungal PG the Gln residue is found. In addition a few important residues adjacent to these clusters were also noted and they were found to differ according to speciation. These residual differences may be important as they cluster around the active site region. Probably these speciation differences may contribute to the specificity of the PGs in various organisms.

3.2. Specificity of tomato PG with PGA and PGM substrates

In tomato PG–octaGalpA complex (Fig. 1), with docked energy 2.41 kcal/mol, the non-reducing end of the substrate is directed towards the N-terminus of the enzyme as suggested by Pages et al. [25]. The glycosidic torsion angles ϕ and ψ and the backbone bond angle $\tau = (C1_i{-}O_{i+1}{-}C4_{i+1})$ of the modeled PGA molecule in the complex are given in Table 2. This conformation of PGA did not show any preference for the 2_1 ($\tau = 117°$, $\phi = 80°$ and $\psi = 161°$) or 3_1 ($\tau = 117°$, $\phi = 80°$ and $\psi = 89°$) helix [26] but has intermediate conformation. The NMR study on the structure of pectate in plant cell wall predicted a complex conformation, containing both 2_1 and 3_1 helices as well as intermediate conformational states [27]. This confirms the reliability of the tomato PG–octaGalpA complex configuration.

The detailed hydrogen bondings and non-bonded interaction mode between the protein and the substrate are shown in Fig. 2(a) and the amino acid residues in the protein within 7 Å distance from the ligand is given in Table 3. The important regions identified from sequence analysis by Pickersgill and coworkers [5] and also by ours are related to functional clustering and found to interact with the PGA molecule. In the Ser225-Ile226-Gly227-Ser228 clustering only Ser228 is found to interact with PGA and in the Arg-Ile-Lys clustering Ile residue does not show interaction in this model. The subsite residues of tomato PG identified based on structural alignment with fungal PG (1czf) are shown in Fig. 3. The residues in the −2, −1, +1 and +2 subsite regions of the tomato PGs are found to interact with the substrate molecule through hydrogen bonding, non-bonded or water mediated interactions. It is surprising to note that the residue Tyr290 at subsite +1 and Gln288 at subsite +2 has no interaction suggesting that the conformation at the reducing end of the substrate has to be re-examined. But conformational changes performed manually at the reducing end of the substrate did not produce any biochemically suitable configuration.

It is interesting to note that in the complex configuration of tomato PG–octaGalpA, His222 makes hydrogen bond with the $GalpA^{+1}$ residue and Asn176 interacting with $GalpA^{+1}$ residue and glycosidic bond between $GalpA^{-1}$–$GalpA^{-2}$. These two hydrogen bonds may probably stabilize the half-chair form of the pyranose ring in $GalpA^{-1}$ residue. The residue His222 is also found to interact through hydrogen bond with the main chain oxygen atom of Asp199. These hydrogen bonded interactions confirm the predicted roles of His222 as distorting the galacturonate residue in subsite −1 [19] and maintaining the proper ionization state of the carboxylate (Asp199) involved in catalysis by sharing a proton [7]. From this model it is also noted that the Asn176 residue is also found to stabilize the conformation of the $GalpA^{-1}$–$GalpA^{+1}$ segment.

The interaction mode of the best model obtained for the methylesterified galacturonic acid is shown in Fig. 2(b), the docked energy being 1.03 kcal/mol. Surprisingly the non-reducing end of the substrate is directed towards the C-terminus of the enzyme and this is in contrary with the PGA complex.

Table 3
The residues of PG that interact with the ligand molecules within 7 Å distance for the docked structures

Plant		Fungi	
PGA	PGM	PGA	PGM
ASP82	PRO112	GLY119	GLY117
TRP111	SER113	THR120	LYS118
PRO112	SER114	LYS127	GLY119
SER113	LYS115	LEU149	THR120
SER114	LYS116	**MET150**	SER121
CYS115	ILE117	HIS177	LYS127
LYS116	ASN118	***ASN178***	ASP172
ILE117	LYS119	**ASP180**	GLY176
ASN118	LYS154	**ASP201**	HIS177
LYS119	SER171	**ASP202**	***ASN178***
PRO122	ALA172	ASN207	**ASP180**
PRO127	LYS173	**HIS223**	**GLN200**
THR128	SER174	**SER226**	**ASP201**
TRP133	PRO175	**GLY228**	ASN207
GLN150	**ASN176**	**SER229**	GLY221
ILE151	**HIS181**	ARG233	**GLY222**
ILE153	SER183	**GLU252**	***HIS223***
LYS154	**GLY198**	ASN253	**SER229**
GLU156	**ASP199**	***ARG256***	GLY231
SER171	VAL205	***LYS258***	ASP232
ALA172	PRO220	ILE260	ARG233
LYS173	**GLY221**	**TYR291**	SER234
SER174	***HIS222***	ASP293	SER249
PRO175	**GLY227**	GLY294	ASN250
ASN176	**SER228**	LYS295	SER251
THR177	GLY230	PRO296	**GLU252**
ASP178	SER231	THR297	ASN253
HIS181	GLY232		**ARG256**
VAL182	ASN233		ILE260
SER183	SER234		GLY279
THR197	GLY250		ILE280
GLY198	**GLU252**		SER281
ASP199	**LYS281**		**ASP282**
ASP200	**THR290**		**TYR291**
SER203	CYS291		GLU292
VAL205	ASP292		ASP293
PRO220	ARG293		GLY294
GLY221	VAL294		LYS295
HIS222			ASP319
GLY227			
SER228			
GLU252			
ARG256			
LYS258			
LYS281			
ASP292			

The residues that are underlined are found in the functional clustering. Bolded ones represent the residues involved in various subsite regions and the residues involved in hydrogen bonding with the substrate are in italics.

Restriction imposed on the PGM molecules to take up similar orientation as that of PGA during docking produced many steric hindrances with PG and so this model was chosen. Only few residues involved in the five functional clustering regions are observed and the residues involved in the −2, −1, +1 and +2 subsite regions are found to interact with the exception of Ile151 in subsite −2 and the catalytic residue Asp200. In this model, His222 residue is hydrogen bonded directly to $GalpA^{-1}$ residue and Asp199. Comparatively this tomato PG–PGM

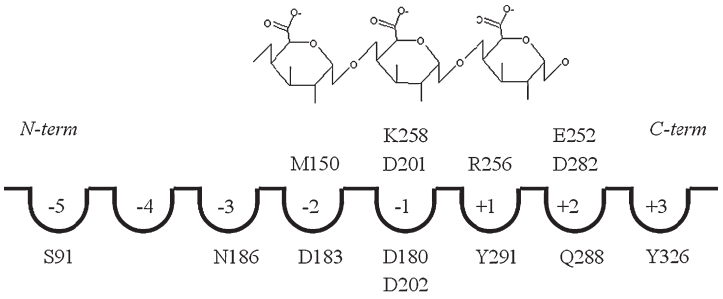

Fungal PG	Tomato PG
S91	A88
M150	I151
D180	D178
D183	H181
N186	N184
D201	D199
D202	D200
E252	E252
R256	R256
K258	K258
D282	K281
Q288	D287
Y291	Y290
Y326	I324

Fig. 3. Subsite map of *A. niger* polygalacturonase with the corresponding tomato PG residues identified by structural alignment.

complex has minimum interactions and also found to bind in the opposite mode (non-reducing towards C-terminus of PG). Since the substrate is bound in the opposite direction and the catalytic residue Asp200 has no interaction, tomato PG cannot hydrolyze PGM and because the interactions are weak when compared with PGA complex strong inhibition of the methylesterified substrate of tomato PG is unlikely. These suggest that tomato PG is specific for PGA and methylesterification of the substrate may not inhibit it.

3.3. Specificity of fungal PG with PGA and PGM substrates

As observed for tomato PG–PGA complex in the docked complex of fungal PG with octaGalpA (docked energy 5.10 kcal/mol) the non-reducing end is directed towards the N-terminus of the fungal PG and the substrate has mixed (2_1 and 3_1 helical) and intermediate conformations. Residues belonging to the five functional clusters are found to interact with the substrate molecule with the exception of one residue in each cluster. Only residues that are proposed to be in the -2, -1 and $+1$ subsites are found in the interaction map of this fungal PG–PGA complex configuration (Fig. 4(a)). The $+2$ subsite residues found in tomato PG–substrate complex are not identified in this model. The residues Asn178, Arg256 and Lys258 found in the subsites -1 and $+1$ are observed to make hydrogen bonds with $GalpA^{-1}$ residue of PGA substrate. These hydrogen bonds stabilize the high energy (half-chair) form of the $GalpA^{-1}$ residue. The residue His223 is not found to make hydrogen bond with the substrate as observed in the tomato PG complex but has non-bonded interactions.

The complex of fungal PG with methylesterified PGA substrate (docked energy 5.24 kcal/mol) is shown in Fig. 1(b) and the non-bonded contacts in Fig. 4(b). The substrate binds in the protein with the non-reducing end towards the C-terminal

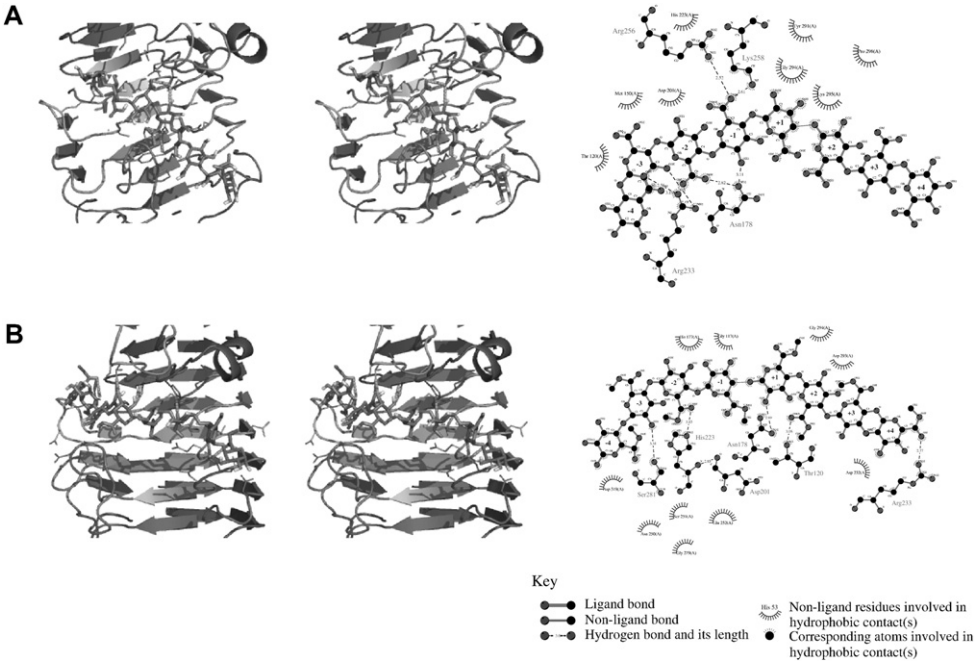

Fig. 4. Stereo plot of the protein (cartoon representation)–ligand (stick representation) complex and their corresponding ligplot showing the detailed interaction mode between the amino acid residues of fungal PG with (A) PGA and (B) PGM residues.

similar to the tomato PG–PGM complex. Most of the residues of the five functional clusters are found to interact with the substrate and the subsite residues of −1, +1 and +2 are also observed to interact. Surprisingly the catalytic residue Asp202 has no interaction as noted in the tomato PG–PGM complex. It is interesting to note that His223 makes hydrogen bond with GalpA^{-2} and Asn178 with GalpA^{+1} similar to the tomato PG–PGA complex. These interactions stabilize the half-chair form of GalpA^{-1} and also maintain the proper ionization state of the Asp200 residue. These interactions produce strong binding of the methylesterified substrate to the fungal PG than the PGA substrate. This predicted fungal PG–PGM complex configuration can explain the inhibition of PG with the methylesterification of the substrate as reported by Dinu [10]. The PGM substrate binds in the opposite direction to the fungal PG and the catalytically important Asp202 residue is not found in the interaction map, which does not allow the methylesterified substrate to hydrolyze and due to the presence of more interactions (than PGA) it binds strongly with the PGM and therefore the inhibition is observed.

4. Conclusion

Octagalacturonic acid and the methylesterified substrate are flexibly docked with the tomato PG and the fungal PG. The important functional regions and the residues are identified in the resultant complexes. The substrate PGA is found to bind with the non-reducing end towards the N-terminus whereas the PGM binds in opposite direction with both complexes. Both PGM complexes did not show the catalytically important Asp residue (200 in tomato and 202 in fungal PG) in the interaction map suggesting strongly the inactiveness of the PGs with the methylesterified substrate. The tomato PG–PGA complex possesses stronger interaction when compared to its methylesterified substrate whereas it is the methylesterified substrate which shows stronger interaction in the fungal PG. This study explains the inhibition of the fungal PG with the methylesterification of the substrate.

Acknowledgement

SMMS acknowledges the financial assistance from Council of Scientific and Industrial Research, Government of India.

Appendix A. Supplementary data

Supplementary data associated with this article can be found in the online version, at doi:10.1016/j.polymer.2006.11.055.

References

[1] Jaubert S, Laffaire J-B, Abad P, Rosso M-N. FEBS Lett 2002;522:109–12.
[2] Henrissat B. Biochem J 1991;280:309–16.
[3] Henrissat B, Bairoch A. Biochem J 1993;293:781–8.
[4] Henrissat B, Bairoch A. Biochem J 1996;316:695–6.
[5] Pickersgill R, Smith D, Worboys K, Jenkins J. J Biol Chem 1998;273:24660–4.
[6] Kester HCM, Kusters-van Someren MA, Muller Y, Visser J. Eur J Biochem 1996;240:738–46.
[7] Armand S, Wagemaker MJM, Sanchez-Torres P, Kester HCM, van Santen Y, Dijkstra BW, et al. J Biol Chem 2000;275:691–6.
[8] Davies GJ, Henrissat B. Structure 1995;3:853–9.
[9] Benen JAE, Kester HCM, Visser J. Eur J Biochem 1999;259:577–85.
[10] Dinu D. Roum Biotechnol Lett 2001;6:397–402.
[11] Coutinho PM, Henrissat B. Carbohydrate-active enzymes: an integrated database approach. In: Gilbert HJ, Davies G, Henrissat B, Svensson B, editors. Recent advances in carbohydrate bioengineering. Cambridge: The Royal Society of Chemistry; 1999. p. 3–12.
[12] Chenna R, Sugawara H, Koike T, Lopez R, Gibson TJ, Higgins DG, et al. Nucleic Acids Res 2003;31:3497–500.
[13] Grierson D, Tucker GA, Keen J, Ray J, Bird CR, Schuch W. Nucleic Acids Res 1986;14:8595–603.
[14] Kabsch W, Sander C. Biopolymers 1983;22:2577–637.
[15] Russell RB, Barton GJ. Proteins 1992;14:309–23.
[16] Biosym/MSI. Insight II user guide. San Diego: Biosym/MSI; 1995.
[17] Schwede T, Kopp J, Guex N, Peitsch MC. Nucleic Acids Res 2003;31:3381–5.
[18] Hooft RW, Sander C, Vriend G. Proteins 1996;26:363–76.
[19] van Santen Y, Benen JAE, Schroter K-H, Kalk KH, Armand S, Visser J, et al. J Biol Chem 1999;274:30474–80.
[20] Cho SW, Lee S, Shin W. J Mol Biol 2001;314:863–78.
[21] Rye CS, Withers SG. Curr Opin Chem Biol 2000;4:573–80.
[22] Morris GM, Goodsell DS, Halliday RS, Huey R, Hart WE, Belew RK, et al. J Comput Chem 1998;19:1639–62.
[23] McDonald IK, Thornton JM. J Mol Biol 1994;238:777–93.
[24] Wallace AC, Laskowski RA, Thornton JM. Protein Eng 1995;8:127–34.
[25] Pages S, Heijne WHM, Kester HCM, Visser J, Benen JAE. J Biol Chem 2000;275:29348–53.
[26] Scavetta RD, Herron SR, Hotchkiss AT, Kita N, Keen NT, Benen JAE, et al. Plant Cell 1999;11:1081–92.
[27] Jarvis MC, Apperley DC. Carbohydr Res 1995;275:131–45.